Supporting Information

Self-Assembled Mesoporous Zeolitic Imidazolate Framework-8 (ZIF-8) Nanocrystals Bearing Thiol Groups for Separations Technologies

Gustavo Manuel Segovia,[a,b] Jimena Soledad Tuninetti,[a] Omar Azzaroni,[a,*] and Matías Rafti[a,*]

a) Instituto de Investigaciones Fisicoquímicas Teóricas y Aplicadas (INIFTA), Fac. de Cs. Exactas, Universidad Nacional de La Plata - CONICET, 64 y Diag. 113, (1900) La Plata, Argentina.

b) Universidad Nacional de San Martín, Argentina.

Corresponding authors: azzaroni@inifta.unlp.edu.ar, mrafti@quimica.unlp.edu.ar

This supporting information contains 10 pages, including description of characterization techniques and figures covering results of the following characterization techniques for μ-ZIF-8+Cys, n-ZIF-8+Cys films: Wide angle X-ray scattering, transmission electron microscopy, Raman vibrational spectroscopy, nitrogen adsorption isotherms, atomic force microscopy, dynamic light scattering, cyclic voltammetry, X-ray photoelectron spectroscopy, atomic force microscopy. This document includes 11 figures, 2 tables, and this cover page.

SD.1 Experimental techniques

SD.1.1 Wide Angle X-ray Scattering

Crystalline structure was determined using wide angle X-ray scattering (WAXS) on powdered samples. The SAXS/WAXS system (INIFTA, "Nanopymes"-EuropeAid/132184 D/SUP/AR Contract 331-896) is a XEUSS 1.0 HR (XENOCS, Grenoble) equipped with a microfocus X-ray source and a Pilatus 100 K detector (DECTRIS AG, Switzerland).

SD.1.2 Dynamic Light Scattering

A Zetasizer Nano ZS apparatus from Malvern was used in order to determine nanocrystal colloids size distribution and polydispersity through in-situ DLS experiments.

SD.1.3 Transmission Electron Microscopy

Transmission Electron Microscopy (TEM) experiments were carried with a LaB6-TEM of type JEOL JEM-1400PLUS equipped with a GATAN US1000 CCD camera.

SD.1.4 X-ray Photoelectron Spectroscopy

XPS experiments were performed in a SPECS Sage HR 100 spectrometer with a non-monochromatic X-ray source (Aluminium Kα line of 1486.6 eV energy and 300 W), placed perpendicular to the analyzer axis and calibrated using the $3d_{5/2}$ line of Ag with a full width at half maximum (FWHM) of 1.

SD.1.5 Raman Spectroscopy

A portable Raman spectrometer with high quantum efficiency CCD array detector and wide dynamic range was used. Measurements were carried for a 65 cm^{-1} to 4200 cm^{-1} wavenumber spectral range, and analyzed with a BWIQ multivariate analysis software and BWID identification software.

SD.1.6 N_2 Adsorption Isotherms

N_2 adsorption isotherms were obtained with a Micrometrics ASAP 2020 surface area and pore size analyzer at 77 K. The adsorption-desorption isotherms were analyzed in order to obtain pore sizes, BET surface areas, and available pore volumes.

SD.1.7 Atomic Force Microscopy

AFM was performed with a Veeco Multimode atomic force microscope attached to a Nanoscope V controller to image the modified gold substrates.

SD.1.8 Electrochemistry

Cyclic Voltammetry (CV) experiments were carried using a Gamry Reference 600 potentiostat, with a three-electrode 2 mL volume Teflon cell. Pt counter electrode and Ag/AgCl (3M NaCl) reference electrode were used. Gold conductive substrates used for film assembly were prepared *via* sputtering.

Reductive electrodesorption thiolate-assembled films. CV experiments were carried using ZIF-8 films, cysteamine SAMs (using cysteamine 10 mM methanolic solutions), and n-ZIF-8+Cys assembled films over gold-coated glass as working electrodes, and buffer aqueous solution of 5 mM HEPES and 100 mM KCl as supporting electrolyte. Experiments were performed under nitrogen atmosphere in order to avoid oxygen electroreduction, as this process can obscure relevant electrochemical features in the applied potential interval of interest.

Evaluation of transport properties of films using redox probe cyclic voltammetry. CV measurements were carried using films assembled with n-ZIF-8+Cys units exposed to different cysteamine contact periods. Scan rates for voltage sweep used were 5, 10, 25, 50, 75, 100, 200 y 500 mV/s with $K_3Fe(CN)_6$ 1 mM / $K_4Fe(CN)_6$ 1 mM concentrations, and 100 mM KCl supporting electrolyte.

SD.2 Figures

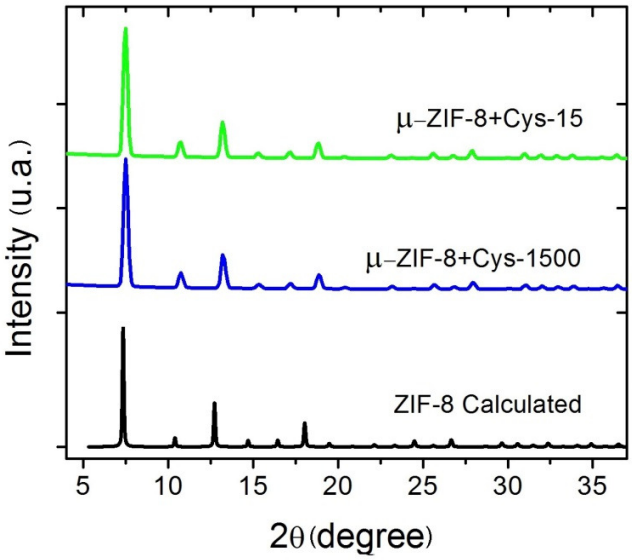

Figure S1. Experimental WAXS patterns for μ-ZIF-8+Cys-15 (green line) and μ-ZIF-8+Cys-1500 (blue line).

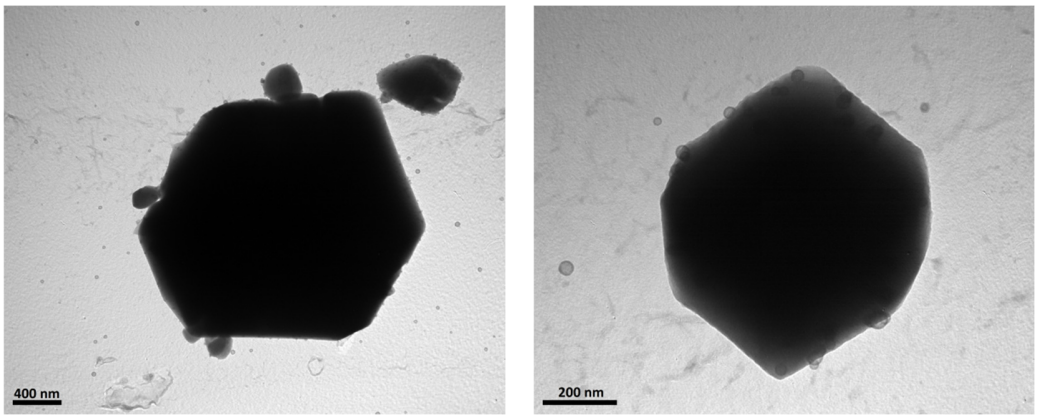

Figure S2. TEM micrographs of μ-ZIF-8+Cys-5.

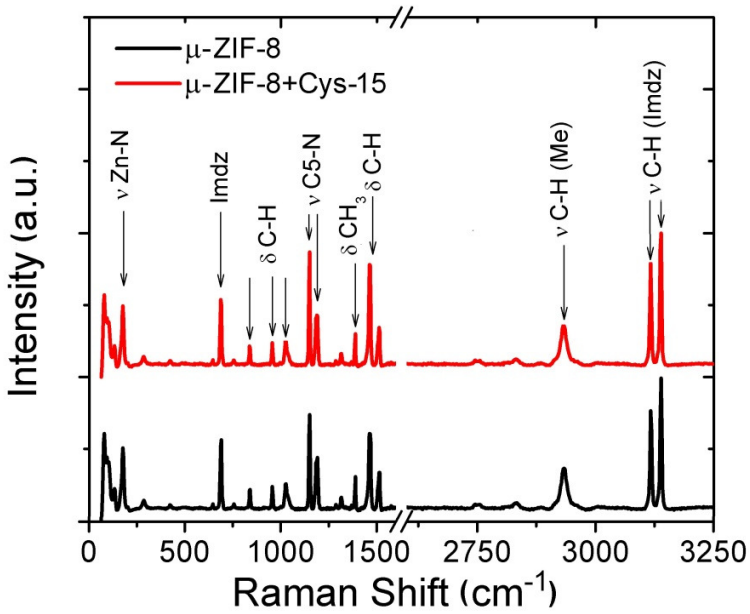

Figure S3. Raman spectra of μ-ZIF-8 (black line) and μ-ZIF-8+Cys (15:1) (red line) with the assignation of most important vibration signals of functional groups composing ZIF-8. The spectra are dominated by intense bands corresponding to methyl group and imidazole ring vibrations. Very strong bands were observed at 172 cm^{-1}, 686 cm^{-1}, 1146 cm^{-1}, 1460 cm^{-1}, 2931 cm^{-1}, 3115 cm^{-1} and 3138 cm^{-1} corresponding to Zn–N stretching, imidazole ring puckering, C5–N stretching, methyl bending, (methyl) C–H stretching and (Imidazole) C–H stretching, respectively. The same signals appear in both spectra suggesting that the modification with cysteamine does not affect the vibrations of the chemical bonds in the nanocrystals and that the amount of the monodentate linker is sufficiently low that vibrations of this last are not observed.

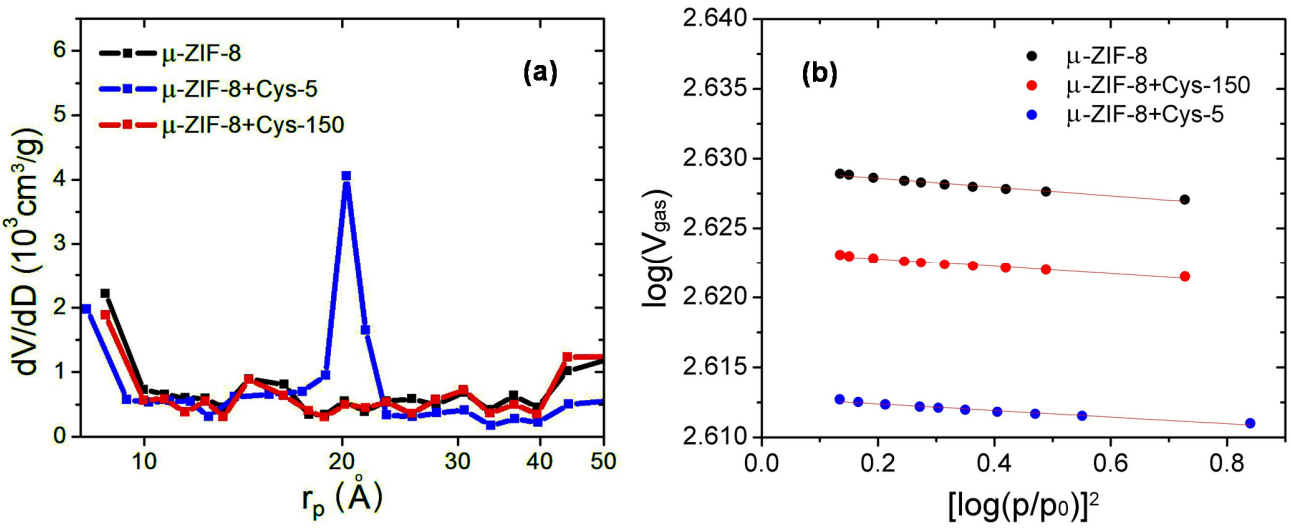

Figure S4. (a) Pore volume distribution obtained through BJH method. (b) Treatment of data of the adsorption isotherms through the Dubinin-Radushkevich equation. Micropore volumes were calculated from each adsorption isotherm, namely, 425.79 cm^3/g, 423.62 cm^3/g and 410.07 cm^3/g for μ-ZIF-8, μ-ZIF-8+Cys (150:1) and μ-ZIF-8+Cys (5:1) respectively.

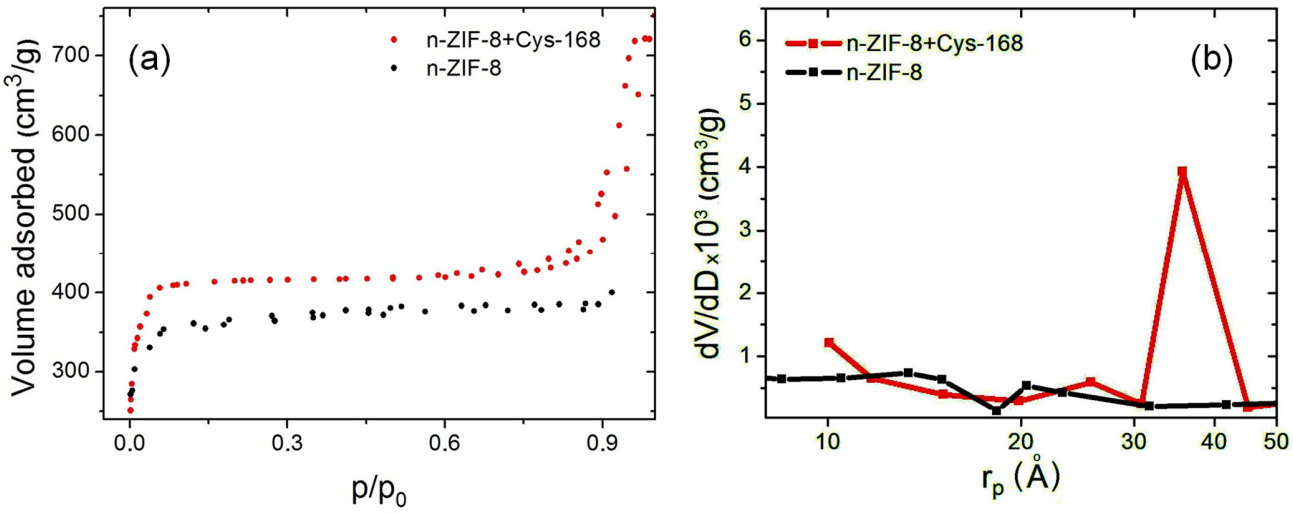

Figure S5. (a) Nitrogen adsorption isotherm of n-ZIF-8+Cys-168 and n-ZIF-8. (b) Comparison of pore volume distribution (obtained through BJH method) of nanocrystals of ZIF-8 (legend shows molar ratio values (150:1), while for n-ZIF-8+Cys-150 corresponds to nanocrystals with exposure time 168 h). Figure S5 (a) shows the nitrogen adsorption isotherm of n-ZIF-8+Cys-168 in which the desorption branch shows a difference, suggesting additional porosity for the mesopores size range (3-4 nm) as can be observed in the figure S5 (b).

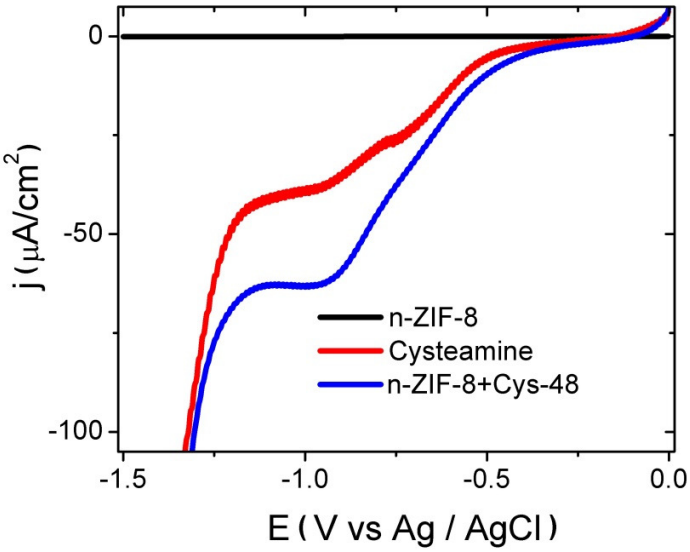

Figure S6. CV experiments carried for films assembled using n-ZIF-8 (black line), a cysteamine Self Assembled Monolayer (red line) and n-ZIF-8+Cys film (blue line, 48 h exposure time) in the potential range where thiolate electrodesorption occurs. The position and intensity of electrodesorption signals are not identical between cysteamine monolayer and the n-ZIF-8+Cys film because of the effect of both, surface concentration and organization of surface structures present.

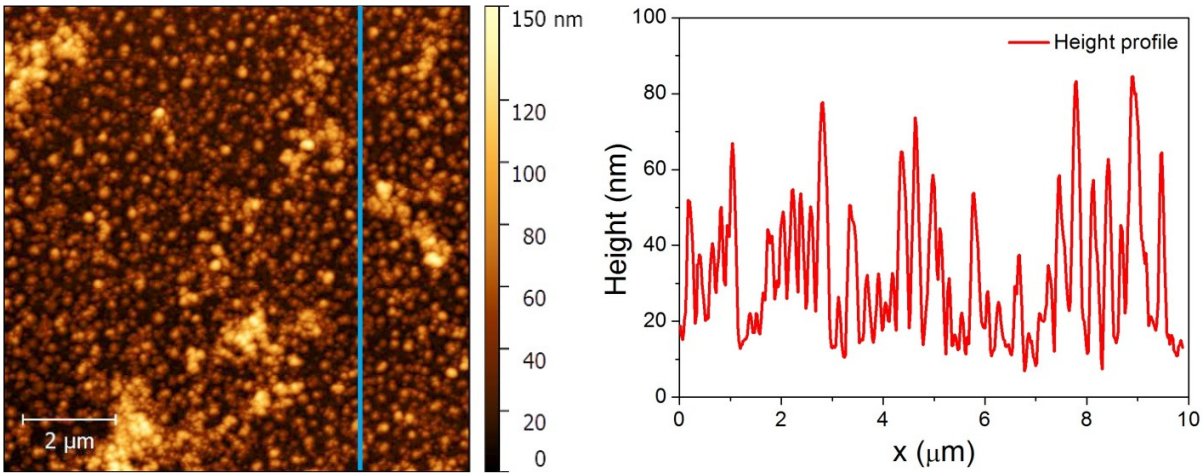

(a) (b)

Figure S7. (a) AFM micrograph and (b) height profile extracted from the light blue straight line in (a).

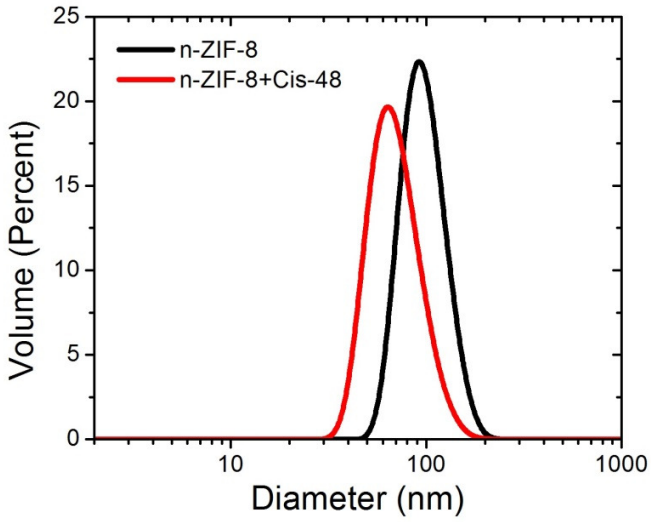

Figure S8. Volume-averaged size distributions obtained by dynamic light scattering (DLS).

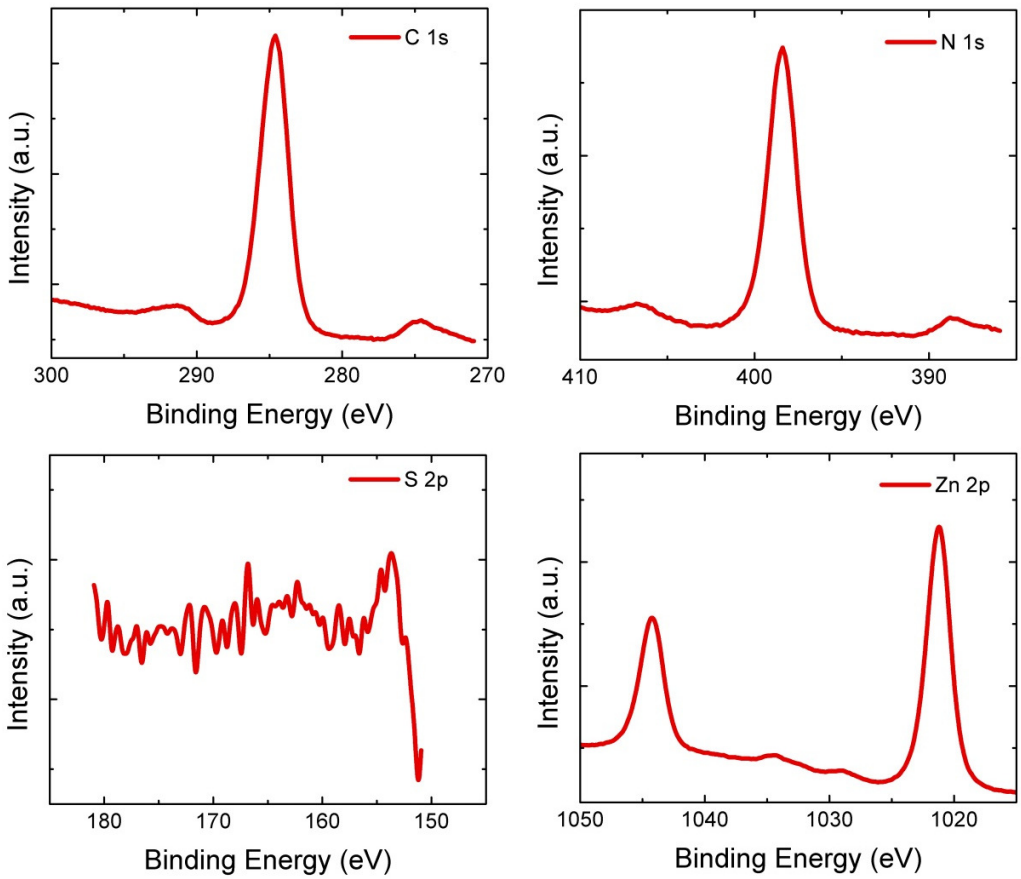

Figure S9. XPS spectra of the energy regions corresponding to the elements composing n-ZIF-8+Cys-48.

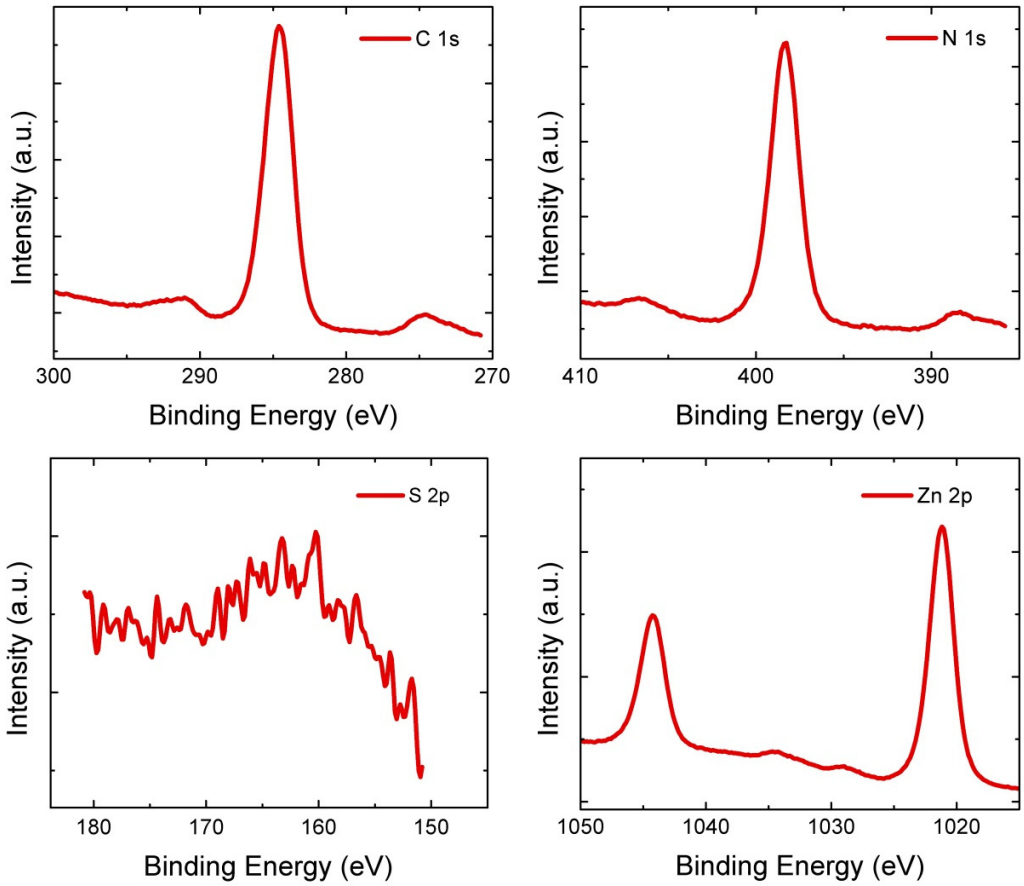

Figure S10. XPS spectra of the energy regions corresponding to the elements composing n-ZIF-8+Cys-168.

Table S1. Summary of the elemental proportions determined through processing of XPS spectra of n-ZIF-8+Cys with exposure times 48 h and 168 h.

	Element	Position (eV)	(S:Zn)
n-ZIF-8+Cys-48	Zn 2p3/2	1021.14	3.80%
	S 2p	160.49	
n-ZIF-8+Cys-168	Zn 2p3/2	1021.16	4.10%
	S 2p	160.26	

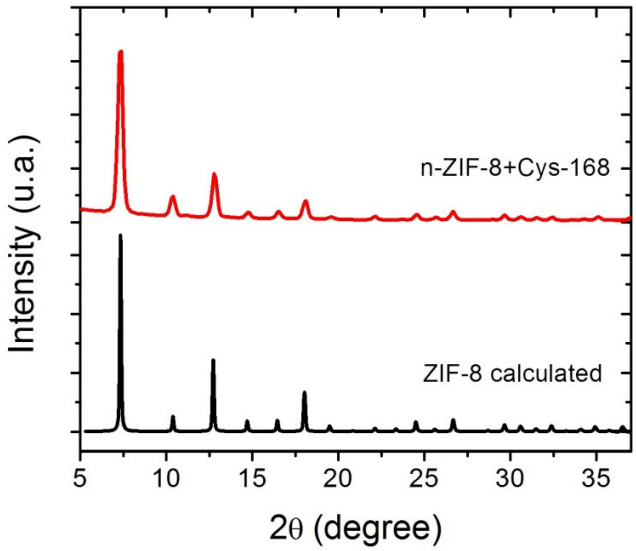

Figure S11. Experimental WAXS pattern for n-ZIF-8+Cys-168 (red line) and calculated ZIF-8(black line).

Table S2. Apparent diffusion coefficients (D_{app}) values obtained from figure 5 in the manuscript.

	n-ZIF-8+Cys-6	n-ZIF-8+Cys-9	n-ZIF-8+Cys-48	n-ZIF-8+Cys-168
D_{app} (cm^2/s)	$4.9x10^{-6}$	$4.3x10^{-6}$	$3.9x10^{-6}$	$3.3\ x10^{-6}$